Supporting Information

Fenton et al. 10.1073/pnas.1715218115

SI Experimental Procedures

Strains, Plasmids, and Routine Growth Conditions. All *Streptococcus pneumoniae* strains in this study were derived from D39 Δ*cps* (1). Cells were grown in THY (Becton Dickinson) at 37 °C in an atmosphere containing 5% CO_2. Strains were grown on prepoured Tryptic Soy Agar 5% sheep blood plates (TSAII 5%SB; Becton Dickinson) with a 5-mL overlay of 1% Nutrient Broth (NB) agar containing additives. When finer control of media components was required, TSA plates containing 5% defibrinated sheep blood were used.

Transposon Insertion Sequencing. Tn-seq was performed as described previously (2, 3) with minor modifications. A total of four independently generated libraries were used in this study: two libraries from *wt* and two from Δ*pbp1a*. Briefly, genomic DNA with Magellan6 transposon insertions was transformed into competent *S. pneumoniae*. Approximately 440,000 (*wt*) and 70,000 (Δ*pbp1A*) transformants were pooled for each library and genomic DNA isolated. Samples were digested with MmeI, followed by adapter ligation. Transposon–chromosome junctions were amplified, gel-purified and sequenced on the Illumina HiSEq. 2500 platform using TruSeq Small RNA reagents (Tufts University Core Facility Genomics). Reads were demultiplexed, trimmed, and transposon-insertion sites mapped onto the D39 genome using methods described in Fenton et al. (4). After normalization, a Mann–Whitney *U* test was used to identify genomic regions with significant differences in transposon insertion profiles. Transposon insertion profiles were visualized using the Artemis genome browser (v10.2) (5). The *wt* vs. Δ*pbp1a* Tn-seq data have been previously published (4) and summarized (with permission) in Fig. S1.

Fluorescence Microscopy. *S. pneumoniae* cells were concentrated by centrifugation at 16,000 × *g* for 1 min and immobilized on pads composed of 2% agarose in 1× PBS. Fluorescence microscopy was performed on a Nikon Eclipse T*i*-E inverted microscope through a Nikon Plan Apo 100× oil objective (NA 1.4). For fluorescent imaging, a SPECTRA X light engine (Lumencor) was used for excitation in combination with the following filter sets for each fluorophore; GFP: Ex:475/28 Em:500–545 Dichroic: 495, for TADA: Ex:438/24 Em:600–660 Dichroic: 595. Images were acquired with a CoolSnapHQ2 CCD camera (Photometrics) without gain using Nikon Elements Software (v4.30). GFP-tagged aPBPs were imaged with a neutral density 8 (ND8) filter with typical acquisition times of 3–5 s. GFP–MacP fusions were imaged without a neutral density filter, with typical acquisition times of 1 s.

Nascent cell wall synthesis was monitored using the Tetramethylrhodamine (TAMRA) TADA dye (Tocris) similar to methods described previously (6, 7). Midexponential cultures (500 μL) were stained with 50 μM TADA for 15 min at 37 °C in a 5% CO_2 atmosphere. Cells were washed with 500 μL PBS to remove unincorporated TADA, concentrated, immobilized on 2% PBS agarose pads, and imaged immediately. Image acquisition times were 50–150 ms.

Image Analysis. For cell-shape analysis of aPBP depletion strains, images were analyzed using the MATLAB-based software packages MicrobeTracker (8) and Oufti (9). Identical parameters were used to identify *S. pneumoniae* cells on both software platforms. Cells were identified using the "analysis" functions and cell dimensions derived from the resulting 2D meshes. Cells were scored independently of developmental stage.

Florescence intensity profiles (Demographs) of GFP and TADA fluorescence signals were generated using Oufti (9). Fluorescence intensity profiles were generated for each cell and were normalized to the region of highest intensity. Normalization reduces signal heterogeneity making localization data within the profiles easier to interpret. Demographs were exported as .EMF files and mounted for figures.

For figures showing individual cells, images were processed using the Metamorph image analysis software (v7.7.0.0). To remove background signal, a region containing no cells was selected and the average signal intensity measured using the regions of interest tool and "Show Region Statistics" functions. This value was deducted from all pixels in the image using the subtraction feature, the resulting images had background pixel intensity values approaching zero and were easier to interpret.

Time-Lapse Microscopy. *S. pneumoniae* cultures were grown to exponential phase in THY at 37 °C in 5% CO_2. 2% agarose pads made with THY were prepared in a Gene Frame (65 μL, 1.5 × 1.6 cm; Thermo Fisher Scientific) and equilibrated at 37 °C for 30 min before use. One-milliliter aliquots of culture were concentrated by centrifugation at 5,000 × *g* for 1 min and cells spotted onto the pad. Time-lapse experiments were performed on a Nikon Eclipse T*i*-E inverted microscope through a Nikon Plan Apo 100× oil objective (NA 1.4) fitted with a heat-collar (Bioptechs), to maintain the pad at 30 °C. After inoculation, pads were placed in contact with the objective and allowed to equilibrate for 30 min before imaging to reduce thermal drift. Images were acquired with a CoolSnapHQ2 CCD camera (Photometrics) using Nikon Elements Software (version 4.30). Images were acquired with reduced illumination (20% lamp voltage) compensated by 4× gain on the CCD. Cells were imaged every 5 min for ∼8 h. Images were aligned using the "Stack Register" function in the Nikon Elements software package. Final figures containing multiple time-lapse series were assembled using ImageJ 1.48v (10), stacked banners added and files exported without compression at 10 frames per second in .avi format.

BACTH Analysis. Competent BTH101 (Δ*cya*) *Escherichia coli* cells were cotransformed with plasmids containing "T25" and "T18" protein fusions. Transformants were selected on LB agar plates containing: 50 μg mL^{-1} ampicillin (Amp^{50}), 25 μg mL^{-1} kanamycin (Kan^{25}), and 40 μg mL^{-1} 5-bromo-4-chloro-3-indolyl-β-D-galactopyranoside ($Xgal^{40}$). Plates were incubated at 30 °C and assessed for signal heterogeneity. Single colonies were picked into 150 μL LB Amp^{50} Kan^{25} containing 500 μg mL^{-1} Isopropyl β-D-1-thiogalactopyranoside ($IPTG^{500}$) in 96 deep-well plates and incubated at 30 °C. Five microliters of each culture was spotted in triplicate onto LB Amp^{50} Kan^{25} $IPTG^{500}$ $Xgal^{40}$ plates. Selected images were representative of three biological replicates.

Immunoblot Analysis. *S. pneumoniae* cultures were normalized to an OD_{600} of 0.3 and 3 mL harvested. Cell extracts were prepared by resuspension of cell pellets in 100 μL lysis buffer (20 mM Tris pH 7.5, 10 mM EDTA, 1 mg mL^{-1} lysozyme, 10 μg mL^{-1} DNase I, 100 μg mL^{-1} RNase A, with protease inhibitors: 1 mM PMSF, 1 μg mL^{-1} leupeptin, 1 μg mL^{-1} pepstatin) and incubation at 37 °C for 10 min, followed by addition of 10 μL 10% Sarcosyl for 5 min. Next, 100 μL SDS sample buffer (0.25 M Tris pH 6.8, 4% SDS, 20% glycerol, 10 mM EDTA) containing 10% 2-mercaptoethanol was added to each prep and samples were heated for 15 min at 50 °C before loading 10 μL per lane. Proteins were separated by SDS/PAGE on 12.5% polyacrylamide gels, electroblotted onto a

PVDF membrane and blocked in 5% nonfat milk in PBS-0.5% Tween-20. The blocked membranes were probed with mouse monocolonal anti-GFP (1:5,000; Sigma) or mouse monocolonal anti-FLAG M2 (1:1,000; Sigma) diluted into 3% BSA in 1× PBS-0.05% Tween-20. Primary antibodies were detected using horseradish peroxidase-conjugated goat anti-mouse IgG (1:10,000; Bio-Rad) and the Western Lightning Plus ECL reagent as described by the manufacturer (PerkinElmer). Membrane chemiluminescence was imaged on a FluorChem R system (ProteinSimple). For immunoblot detection of StkP substrates, an antiphosphothreonine polyclonal antibody (1:2,000, #9381; Cell Signaling) was used in conjunction with a secondary goat anti-rabbit secondary antibody HRP conjugate (1:5,000; Bio-Rad), as described previously (11).

Protease Protection Assay. The *S. pneumoniae* strain Spn326 (Δ*pbp1a* Δ*macP*::P_{fuc}-*gfp-macP*) was grown in 25 mL THY in the presence of 0.4% fucose at 37 °C in 5% CO_2. Exponentially growing cultures (OD_{600} = 0.5) were harvested by centrifugation at 5,000 × *g* for 5 min. Cell pellets were washed in 25 mL SMM (0.5 M sucrose, 20 mM maleic acid, 20 mM $MgCl_2$, pH 6.5) and resuspended in 2 mL SMM. Protoplasts were generated by enzymatic digestion of the cell wall with 5 mg mL^{-1} lysozyme, washed and resuspended in 1 mL SMM. Next, 100-μL aliquots of protoplasts were treated with 15 μL of Proteinase K (50 μg mL^{-1} final concentration in SMM), 15 μL of Proteinase K and Triton X-100 (50% in SMM), or 15 μL SMM alone and incubated for 20 min at room temperature. Proteolysis was halted by the addition of 100 μL 2× SDS/PAGE sample buffer (0.25 M Tris pH 6.8, 4% SDS, 20% glycerol, 10 mM EDTA, 10% 2-mercaptoethanol) and 2 mM of the serine-protease inhibitor PMSF. Samples were denatured for 15 min at 50 °C before loading 10 μL per lane. Proteins were separated by SDS/PAGE on 12.5% polyacrylamide gels, electroblotted onto a PVDF membrane and blocked in 5% nonfat milk in PBS-0.5% Tween-20. The blocked membranes were probed with: anti-FtsH (1:20,000), anti-FtsE (1:20,000), or affinity-purified anti-GFP (1:10,000) rabbit polyclonal antibodies diluted into 3% BSA in 1× PBS-0.05% Tween-20 (12). Primary antibodies were detected using horseradish peroxidase-conjugated goat anti-rabbit IgG (1:20,000; Bio-Rad) and the Western Lightning Plus ECL as described by the manufacturer (PerkinElmer). Membrane chemiluminescence was imaged on a FluorChem R system (ProteinSimple).

Coimmunoprecipitation Assay. Coimmunoprecipitation assays were carried out as described previously (4) using strains: Spn710 (GFP–PBP2a, FLAG–MacP), Spn712 (PBP2a, FLAG–MacP), Spn708 (GFP–PBP1a, FLAG–MacP), Spn797 [GFP–PBP2a, FLAG–MacP(T32A)], and Spn800 [GFP–PBP2a, FLAG–MacP(T32E)]. Monocolonal anti-GFP (1:5,000; Sigma) and anti-FLAG M2 (1:1,000; Sigma) antibodies were used for the detection of GFP–PBP1a, GFP–PBP2a, and FLAG–MacP, respectively. Primary antibodies were detected using horseradish peroxidase-conjugated goat anti-mouse IgG (1:10,000; Bio-Rad) and imaged on a FluorChem R system (ProteinSimple).

Phylogenetic Analysis. MacP homologs were identified using the National Center for Biotechnology Information (NCBI) BLASTp. The *S. pneumoniae* MacP sequences were used as queries against a database of bacterial genomes with an e-value cut-off of 1×10^{-4}. BLAST analysis was carried out using the Harvard Medical School research computing cluster Orchestra (https://rc.hms.harvard.edu/#orchestra).

To search for more distant MacP homologs, we first identified homologs using iterative BLASTP from BLAST package 2.2.6 (13) against a local database containing 4,466 prokaryotic complete proteomes retrieved from NCBI ftp (ftp://ftp.ncbi.nlm.nih.gov/) (Dataset S1). The MacP amino acid sequence from the *S.pneumoniae* R6 sequence was used as the first seed (e-value < 1.0). Homologs were aligned using MAFFT v7.123b (14) to build an HMM profile using HMMER v3.1b1 (15). The profile was then used to query the database with HMMSEARCH from the HMMER package. Additional rounds of HMMSEACH were performed to improve the sensitivity of homolog detection. Given the small size of MacP and the sequence divergence between homologs, the genomic context of each hit (e-value < 10) was examined using GeneSpy (https://lbbe.univ-lyon1.fr/GeneSpy/). Only genes presenting the same genomic context as *S. pneumoniae macP* were considered homologs. Phylogeny of Lactobacillales was inferred from a supermatrix of ribosomal proteins extracted from RiboDB (16). One strain per genus was selected to represent each genus in Lactobacillales. The sequences were aligned using MAFFT (L-INS-I option) and trimmed using BMGE-1.1 (option BLOSUM30) (17). The evolution model was chosen using BIC criteria implemented in Iqtree (18) and the phylogeny was inferred using PhyML (19) (LG+I+F+G4, 13 sequences, 6,027 positions). The trees in Fig. S9 were generated using the Interactive Tree Of Life (v3) web-based tool (itol.embl.de/) (20) and iTOL (21), respectively.

Strain Construction.

S. pneumoniae *deletion strains.* All *S. pneumoniae* deletion strains were generated using linear PCR fragments as described in Fenton et al., (4). Briefly, two ∼1-kb flanking regions of each gene were amplified and an antibiotic resistance marker placed between them using isothermal assembly (22). Assembled PCR products were transformed directly into *S. pneumoniae* as described previously (4). In all cases, deletion primers were given the typical name: "gene-designation"_5FLANK_F/R for 5′ regions and "gene-designation"_3FLANK_F/R for 3′ regions, antibiotic markers were amplified from Δ*bgaA* strains using the AntibioticMarker_F/R primers (AKF_Spn001-005). A full list of primer sequences can be found in the Table S1. Extracted gDNA from deletions strains was confirmed by diagnostic PCR using the AntibioticMarker_R primer in conjunction with a primer binding ∼100 bp 5′ of the disrupted gene; these primers were given the typical name: "ORFdesignation"_Seq_F.

***P_{zn}*-pbp2a.** The P_{czc} promoter (23), henceforth known as P_{zn}, was amplified from pJW025 (24) using primers: oSP104 and oSp105. The *pbp2a* ORF was amplified from the D39 genome using oSp108 and oSp109 and added to the first fragment by isothermal assembly. The resulting construct was digested with BamHI and XhoI and ligated into pLEM019 cut with the same enzymes. This resulted in the plasmid pAKF200, which contains the *pbp2a* ORF under the control of a zinc-inducible promoter with a consensus RBS. This construct was integrated into the D39 genome at the *bgaA* site using flanking regions of homology present in the pLEM019 vector. The P_{zn}-*pbp2a* construct was fully sequenced, linearized, and transformed into *S. pneumoniae* for *bgaA* integration.

***P_{zn}*-gfp-pbp2a.** The whole pAKF200 plasmid was amplified using primers: PBP2a_GFP_F and PBP2a_GFP_R. This introduced both overlapping regions of homology for isothermal assembly and a short linker sequence (coding: LEGPAGL). The *gfp* ORF was amplified using primers: GFP_N_F and GFP _N_R from pUC57-*gfp*. These two fragments were combined by isothermal assembly, resulting in pAKF228. This plasmid was sequenced and transformed into *S. pneumoniae.* Specific integration into *bgaA* locus was confirmed by diagnostic PCR using the BgaA_FLANK_F primer.

***P_{fucose}*-macP.** The *macP* ORF, with its native RBS, was amplified from the D39 genome using primers: spd0876_ nativeRBS_F and spd0876_R. The resulting PCR product was digested with XhoI and BamHI and ligated into pAKF205 cut with the same enzymes. This resulted in the plasmid pAKF204, which contains the *macP* ORF under the control of a fucose-inducible promoter with its native RBS.

P_{fucose}-gfp-macP. The P_{fucose}-*gfp-macP* construct was generated by isothermal assembly. The pAKF204 plasmid was amplified using primers: spd0876_ GFP_F and spd0876_GFP_R. This introduced both overlapping regions of homology for isothermal assembly and a short linker sequence (coding: LEGPAGL). The *gfp* ORF was amplified using primers: GFP _N_F and GFP_N_R from pUC57-*gfp*. These two fragments were combined by isothermal assembly, resulting in pAKF230. The P_{fucose}-*gfp-macP* construct was fully sequenced and transformed into *S. pneumoniae*. Site specific integration into the genome at *bgaA* was confirmed by diagnostic PCR using the bgaA_FLANK_F primer.

GFP–MacP Truncations. Truncations were generated from the P_{fucose}-*gfp-macP* construct (pAKF230). After modification, all constructs were sequenced using the primers: pLEM019_seq_F and GFP_N_R.

P_{fucose}*-gfp-macP *(soluble). For expression of the GFP–MacP(soluble) fusion protein, the primers: pAKF230_Soluble_F and pAKF230_Soluble_R were used to amplify and modify the plasmid pAKF230. Primers amplified the entire plasmid excluding the *macP* coding region between amino acids 85–104 and adding a stop codon after position 85. Primers introduced a BamHI site, which was used to circularize the plasmid before transformation into an *E. coli* cloning strain, the resulting plasmid was named pAKF231.

P_{fucose}*-gfp-macP *(TM region only). For expression of the GFP–MacP(TM only) fusion protein, the primers: pAKF230_TM_F and pAKF230_TM_R were used to amplify and modify the plasmid pAKF230. Primers amplified the entire plasmid excluding the *macP* coding region between amino acids 1–85. Primers introduced a BamHI site, which was used to circularize the plasmid before transformation into an *E. coli* cloning strain, the resulting plasmid was named pAKF234.

***P_{Zn}-FLAG*-macP.** The FLAG-MacP expression construct was generated through isothermal assembly of two PCR products. The first, encoding the *macP* ORF and linker region, was amplified from *wt* gDNA using primers: spd0876_FLAG_F and spd0876_FLAG_R. This was combined with the pAKF227 plasmid backbone PCR amplified using primers: pAKF227_F and pAKF227_R. After assembly, the resulting plasmid expressed an N-terminal triple-FLAG tagged MacP fusion protein upon zinc induction. The FLAG tag and MacP were separated by a linker sequence encoding the amino acids: LEGPAGL. The resulting plasmid was sequenced and named pAKF229.

P_{Zn}-FLAG-MacP phosphorylation variants (T32A and T32E). MacP T32A and T32E substitutions were introduced into the plasmid pAKF229 (P_{Zn}-FLAG-*macP*) using primer pairs: *spd0876*_T32A_F/*spd0876*_T32X_R (for T32A) and *spd0876*_T32E_F/*spd0876*_T32X_R (for T32E) by quick change PCR. Primers sequences substituted the 32nd codon ACT (Thr) for either a GCT (Ala) codon or GAA (Glu) codon. The resulting plasmids pAKF304 and pAKF305 were transformed into *S. pneumoniae* strains.

P_{fucose}-GFP-MacP phosphorylation variants (T32A and T32E). MacP T32A and T32E substitutions were introduced into plasmids: pAKF230 (P_{fucose}-*gfp-macP*) using primer pairs: *spd0876*_T32A_F/*spd0876*_T32X_R (for T32A) and *spd0876*_T32E_F/*spd0876*_T32X_R (for T32E) by quick-change PCR. Primers sequences substituted the 32nd codon ACT (Thr) for either a GCT (Ala) codon or GAA (Glu) codon. The resulting plasmids, pAKF301 and pAKF302 were fully sequenced and transformed into *S. pneumoniae* strains.

Integration of MacP Fusions at the Native Locus. For integration of all *macP* fusions and truncations into the *S. pneumoniae* genome at the native locus, each expression construct was amplified from plasmids using primers: pLEM023_F and pLEM23_R. These primers recognize flanking regions found in all "pAKF" plasmids used in this study and could be used universally for all construct amplifications. The resulting products were combined with a 5′ flanking sequence amplified from *wt* gDNA using primers spd0876_5FLANK_F/spd0876_5FLANK_R and a spectinomycin resistance cassette fused to 3′ flanking sequence amplified from Δ*macP*::*spec* gDNA using primers AntibioticMarker_F/spd0876_3FLANK_R. The three PCR products were combined using isothermal assembly and the resulting assembled product (5′flank-[*macP* expression construct]::*spec*-3′ flank) was transformed into the Δ*macP*::*erm* strain. Transformants were selected on spectinomycin and tested for marker replacement. Strains were verified by diagnostic PCR and detection of the expected fusion protein by immunoblot.

Unmarked *ΔmacP*, *macP(T32A)*, and *macP(T32E)* Strains. For strains analyzed by antiphosphothreonine immunoblot (Fig. 5*A*), the *macP*-null, *macP*(T32A), and *macP*(T32E) mutants were generated using the *Janus* Kan-rpsL cassette (25). This was first inserted at the 3′ end of the chromosomal *macP* gene. For that, a DNA fragment obtained by PCR amplification using primers: 1202/1519 and 1204/1205 was transformed in the D39Δ*cps* strain resulting in the D39Δ*cps macP-kan-rpsL* strain. *macP* and *Janus* were then removed upon transformation with a DNA fragment obtained with primer pairs 1202/1223 and 1224/1205 generating the unmarked D39Δ*cps* Δ*macP* strain.

The unmarked D39Δ*cps macP*(T32A) strain was obtained by transformation of D39Δ*cps macP-kan-rpsL* using a DNA fragment resulting from PCR amplification with primers: 1202/1271. The unmarked D39Δ*cps macP*(T32E) strain was obtained using the same approach with primers: 1202/1272.

BACTH Plasmid Construction. The *macP* ORF was amplified using primers: SPD0876_BTH_N_F/R for N-terminal fusions and SPD0876_BTH_C_F/R for C-terminal fusions. For N-terminal fusions, primers introduced XbaI sites and EcoRI for cloning into the two-hybrid vectors pKT25 and pCH364 digested with the same enzymes. For C-terminal fusions, primers introduced HindIII and BamHI sites for insertion into two hybrid vectors: pKNT25 and pCH363 cut with the same enzymes. The *macP* ORF fusions were fully sequenced before use in the two-hybrid assay.

BACTH Plasmid Construction, MacP T32 Variants. For introducing T32A or T32E substitutions into the *macP* ORF, the primer pairs: *spd0876*_T32A_F/*spd0876*_T32X_R (for T32A) and *spd0876*_T32E_F/*spd0876*_T32X_R (for T32E) were used to modify the pKT25-*macP* plasmid by quick change PCR. Primers sequences substituted the 32nd codon ACT (Thr) for either a GCT (Ala) codon or GAA (Glu) codon. The resulting plasmids were sequenced before use in the two-hybrid assay.

1. Lanie JA, et al. (2007) Genome sequence of Avery's virulent serotype 2 strain D39 of *Streptococcus pneumoniae* and comparison with that of unencapsulated laboratory strain R6. *J Bacteriol* 189:38–51.
2. van Opijnen T, Camilli A (2010) Genome-wide fitness and genetic interactions determined by Tn-seq, a high throughput massively parallel sequencing method for microorganisms. *Curr Protoc Microbiol* Chapter 1:Unit 1E.3.
3. van Opijnen T, Bodi KL, Camilli A (2009) Tn-seq: High-throughput parallel sequencing for fitness and genetic interaction studies in microorganisms. *Nat Methods* 6:767–772.
4. Fenton AK, Mortaji LE, Lau DTC, Rudner DZ, Bernhardt TG (2016) CozE is a member of the MreCD complex that directs cell elongation in *Streptococcus pneumoniae*. *Nat Microbiol* 2:16237.
5. Carver T, Harris SR, Berriman M, Parkhill J, McQuillan JA (2012) Artemis: An integrated platform for visualization and analysis of high-throughput sequence-based experimental data. *Bioinformatics* 28:464–469.
6. Boersma MJ, et al. (2015) Minimal peptidoglycan (PG) turnover in wild-type and PG hydrolase and cell division mutants of Streptococcus pneumoniae D39 growing planktonically and in host-relevant biofilms. *J Bacteriol* 197:3472–3485.
7. Kuru E, et al. (2012) In situ probing of newly synthesized peptidoglycan in live bacteria with fluorescent D-amino acids. *Angew Chem Int Ed Engl* 51:12519–12523.
8. Sliusarenko O, Heinritz J, Emonet T, Jacobs-Wagner C (2011) High-throughput, subpixel precision analysis of bacterial morphogenesis and intracellular spatio-temporal dynamics. *Mol Microbiol* 80:612–627.
9. Paintdakhi A, et al. (2016) Oufti: An integrated software package for high-accuracy, high-throughput quantitative microscopy analysis. *Mol Microbiol* 99:767–777.
10. Schneider CA, Rasband WS, Eliceiri KW (2012) NIH image to ImageJ: 25 years of image analysis. *Nat Methods* 9:671–675.

11. Fleurie A, et al. (2012) Mutational dissection of the S/T-kinase StkP reveals crucial roles in cell division of *Streptococcus pneumoniae*. *Mol Microbiol* 83:746–758.
12. Meisner J, et al. (2013) FtsEX is required for CwlO peptidoglycan hydrolase activity during cell wall elongation in *Bacillus subtilis*. *Mol Microbiol* 89:1069–1083.
13. Altschul SF, et al. (1997) Gapped BLAST and PSI-BLAST: A new generation of protein database search programs. *Nucleic Acids Res* 25:3389–3402.
14. Katoh K, Standley DM (2013) MAFFT multiple sequence alignment software version 7: Improvements in performance and usability. *Mol Biol Evol* 30:772–780.
15. Eddy SR (2009) A new generation of homology search tools based on probabilistic inference. *Genome Inform* 23:205–211.
16. Jauffrit F, et al. (2016) RiboDB database: A comprehensive resource for prokaryotic systematics. *Mol Biol Evol* 33:2170–2172.
17. Criscuolo A, Gribaldo S (2010) BMGE (block mapping and gathering with entropy): A new software for selection of phylogenetic informative regions from multiple sequence alignments. *BMC Evol Biol* 10:210.
18. Nguyen LT, Schmidt HA, von Haeseler A, Minh BQ (2015) IQ-TREE: A fast and effective stochastic algorithm for estimating maximum-likelihood phylogenies. *Mol Biol Evol* 32:268–274.
19. Guindon S, et al. (2010) New algorithms and methods to estimate maximum-likelihood phylogenies: Assessing the performance of PhyML 3.0. *Syst Biol* 59:307–321.
20. Letunic I, Bork P (2016) Interactive tree of life (iTOL) v3: An online tool for the display and annotation of phylogenetic and other trees. *Nucleic Acids Res* 44:W242-5.
21. Letunic I, Bork P (2007) Interactive tree of life (iTOL): An online tool for phylogenetic tree display and annotation. *Bioinformatics* 23:127–128.
22. Gibson DG, et al. (2009) Enzymatic assembly of DNA molecules up to several hundred kilobases. *Nat Methods* 6:343–345.
23. Kloosterman TG, van der Kooi-Pol MM, Bijlsma JJE, Kuipers OP (2007) The novel transcriptional regulator SczA mediates protection against Zn2+ stress by activation of the Zn2+-resistance gene czcD in *Streptococcus pneumoniae*. *Mol Microbiol* 65: 1049–1063.
24. Eberhardt A, Wu LJ, Errington J, Vollmer W, Veening JW (2009) Cellular localization of choline-utilization proteins in *Streptococcus pneumoniae* using novel fluorescent reporter systems. *Mol Microbiol* 74:395–408.
25. Sung CK, Li H, Claverys JP, Morrison DA (2001) An rpsL cassette, Janus, for gene replacement through negative selection in *Streptococcus pneumoniae*. *Appl Environ Microbiol* 67:5190–5196.

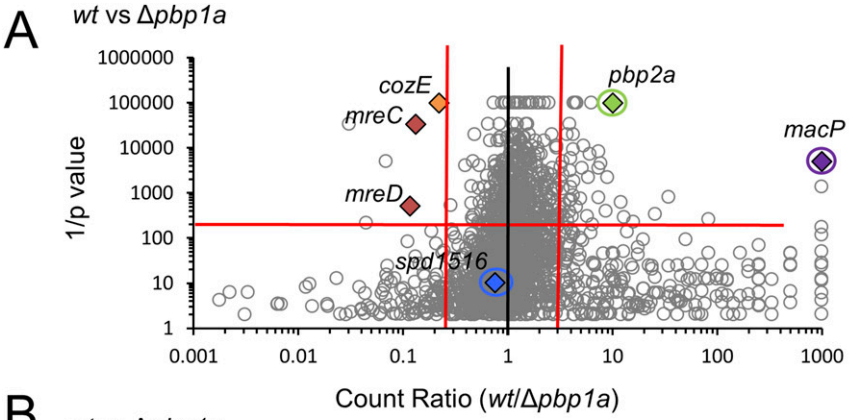

B

wt vs Δpbp1a

Locus Name	Number of TA sites in ORF	Count Ratio (*wt*/Δ*pbp1a*)	U stat	p-value
macP (*spd0876*)	21	'1000'	115	0.0002
pbp2a	145	10	3814	0.00
cozE	112	0.22	4507	0.00
mreC	63	0.12	1592	0.0019
mreD	49	0.13	745	0.00003
spd1516	69	0.75	2081	10.34

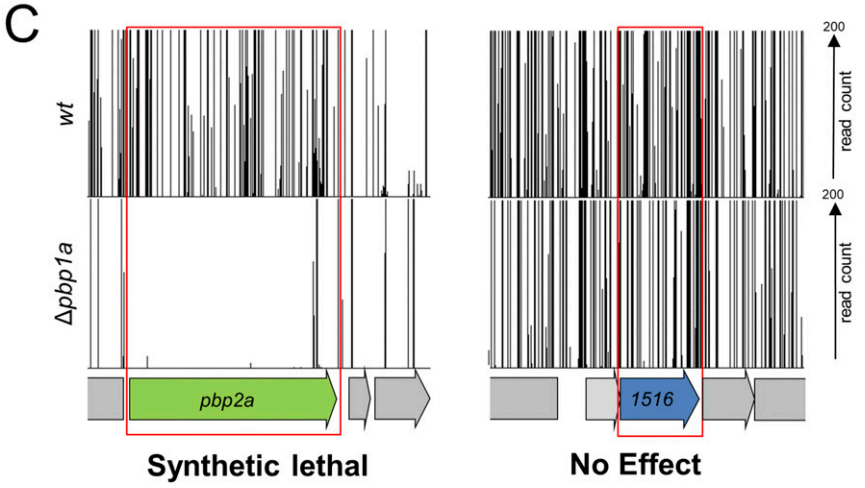

Fig. S1. Tn-Seq analysis comparing wild-type and Δpbp1a transposon libraries. (*A*) An inversed volcano plot comparing *wt* and Δ*pbp1a* Tn-seq data. Red lines indicate cut-off values used by this study to identify hits in the screen, $P < 0.0005$ and count ratio > sevenfold. The *macP* ORF is highlighted in purple. Examples of a known synthetic lethal gene (*pbp2a*), synthetic viable genes (*mreCD* and *cozE*) and an ORF not essential in either library (*spd1516*) are also highlighted. (*B*) Table showing *wt* vs. Δ*pbp1a* Tn-Seq output statistics of the ORFs highlighted in *A*. A Mann–Whitney *U* test is used to define significant differences in transposon insertion profiles across each ORF. (*C*) Representative transposon insertion profiles for *pbp2a* and gene *spd1516*. Transposon insertions in *pbp2a* are dramatically underrepresented in the Δ*pbp1a* library compared with wild-type. In contrast, no significant difference in transposon insertions is observed for *spd1516*. This figure was modified from Fenton et al. (1) to highlight the *macP* ORF and place it in context with the whole Δ*pbp1a* Tn-seq dataset.

1. Fenton AK, Mortaji LE, Lau DTC, Rudner DZ, Bernhardt TG (2016) CozE is amember of the MreCD complex that directs cell elongation in Streptococcus pneumoniae. *Nat Microbiol* 2:16237.

A

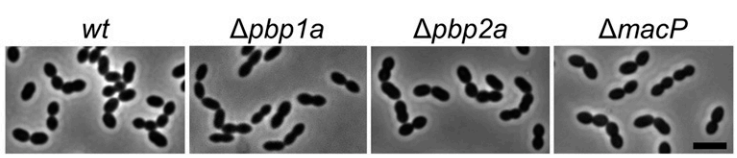

B

	wt	Δpbp1a	Δpbp2a	ΔmacP
Average Length (μm)	2.27 (± 0.41)	2.22 (± 0.43)	2.19 (± 0.44)	2.17 (± 0.42)
Average Width (μm)	0.87 (± 0.05)	0.82 (± 0.04)	0.86 (± 0.04)	0.86 (± 0.04)
'Aspect Ratio' (Length/width)	2.61 (± 0.37)	2.72 (± 0.45)	2.53 (± 0.44)	2.52 (± 0.42)

C

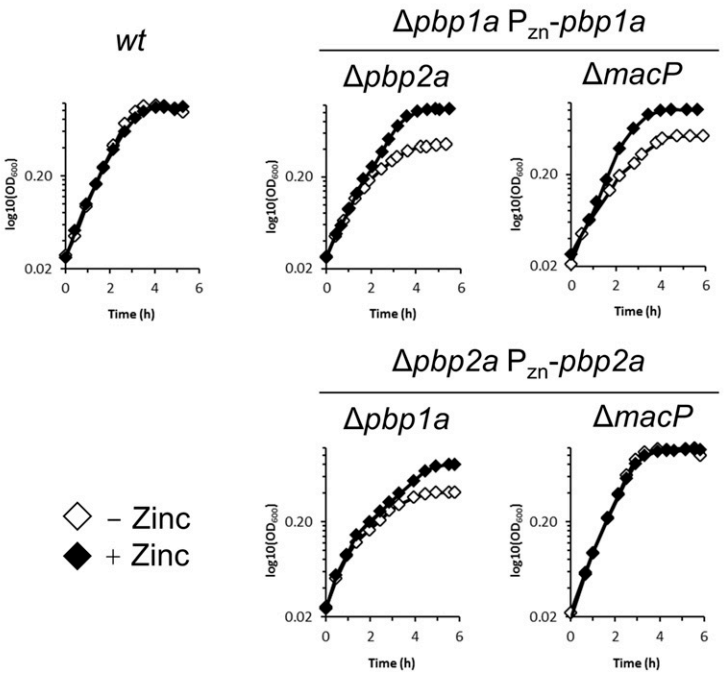

Fig. S2. Cells lacking essential aPBP activity experience growth arrest before lysis. (*A*) Cells individually lacking PBP1a, PBP2a, or MacP are morphologically similar to wild-type. Representative images of *wt*, Δ*pbp1a*, Δ*pbp2a*, and Δ*macP* deletion strains. Strains were grown in THY at 37 °C in 5% CO_2 to mid-exponential phase. Cells were imaged on a THY 2% agarose pad, $n = 4$. (Scale bar, 3 μm.) (*B*) Quantitative analysis of cell dimensions for strains lacking PBP1a, PBP2a, or MacP. Although not significant, a modest (5%) reduction in average cell width was observed for the Δ*pbp1a* strain compared with *wt*. 300 cells were scored per strain, 150 in each biological replicate, $n = 2$, numbers in parentheses indicate SD of the whole population. (*C*) Representative growth curves for aPBP depletion strains in the presence and absence of inducer. The indicated strains were grown in THY to midexponential phase, diluted into fresh THY to an OD_{600} of 0.025 in the presence or absence of 200 μM $ZnCl_2$ and incubated at 37 °C with 5% CO_2. OD_{600} was measured approximately every 30 min for 6 h. Growth curves are representative of three replicates. Strains depleted of essential aPBP activity did not increase in optical density above 0.3. Depletion of PBP2a in the strain lacking MacP is shown to highlight the growth arrest phenotype is specific to cells lacking PBP1a.

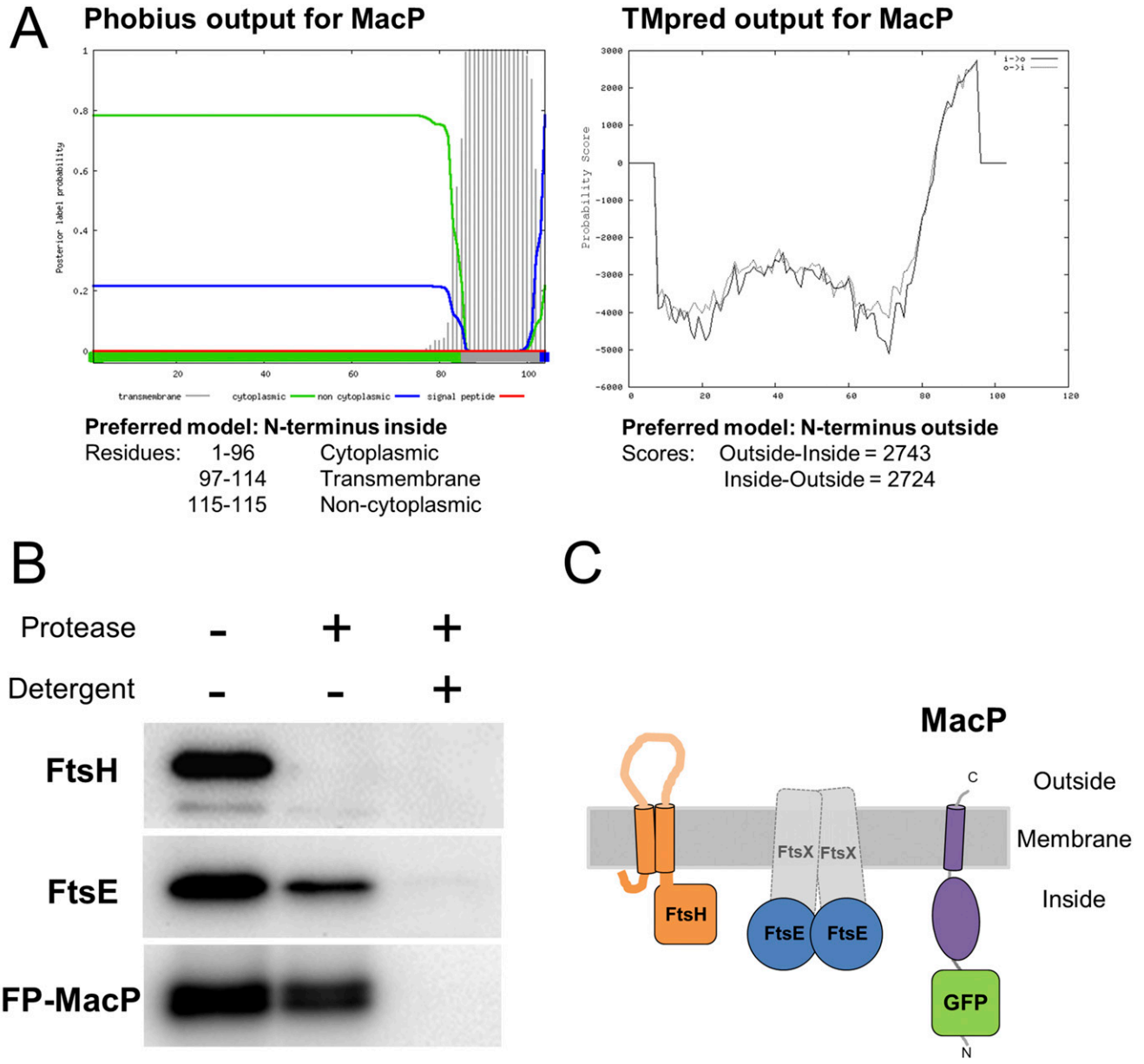

Fig. S3. Topological analysis of MacP. (*A*) Output from the Phobius and TMpred web servers for MacP topology. Predicted topology and probability scores generated by the software are shown below each graph. Phobius can be found at: (phobius.sbc.su.se/) (1) and TMpred at: (embnet.vital-it.ch) (2). (*B*) Immunoblots from protease accessibility assay. Protoplasts of a *S. pneumoniae* strain harboring a functional GFP–MacP fusion were treated with proteinase K with or without 1% Triton X-100 or untreated. The membrane protein FtsH and the soluble protein FtsE were used as positive and negative controls, respectively. (*C*) Schematic diagram of topologies of FtsH, FtsE, and MacP. The topology of FtsH is based on predictions using the Phobius web server. The membrane protein FtsX is shown in complex with FtsE.

1. Käll L, Krogh A, Sonnhammer ELL (2004) A combined transmembrane topology and signal peptide prediction method. *J Mol Biol* 338:1027–1036.
2. Hofmann K, Stoffel W (1993) TMbase-a database of membrane spanning proteins segments. *Biol Chem Hoppe Seyler* 347:166.

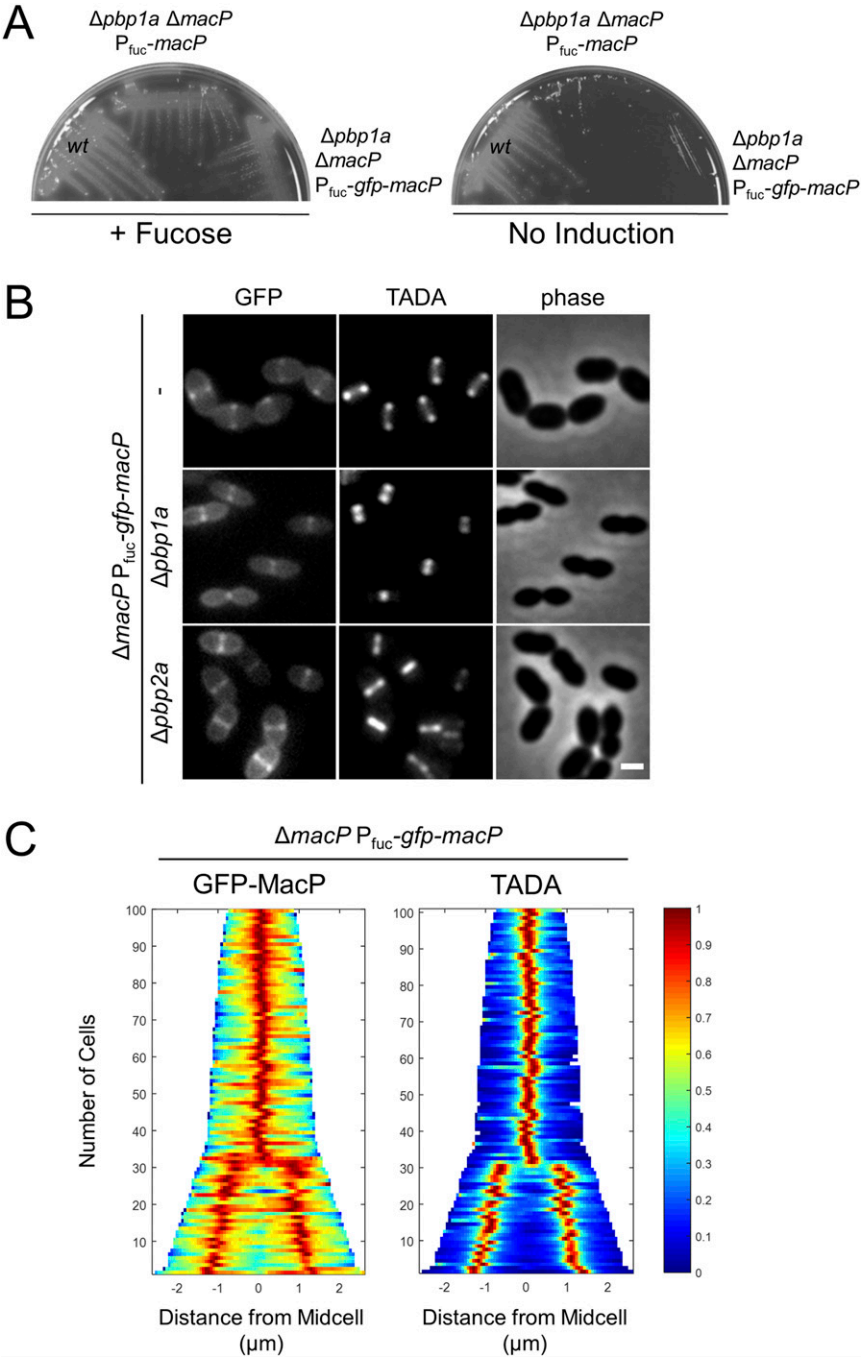

Fig. S4. GFP–MacP is enriched at midcell. (*A*) The GFP–MacP fusion protein complements the Δ*pbp1a* Δ*macP* synthetic lethality. Depletion strains contain *macP* or *gfp-macP* fused to a fucose-inducible promoter (P_{fuc}). Strains AKF_Spn290, 326 and a wild-type control were streaked on TSAII 5%SB overlay plates with either 0.4% fucose or 0.4% sucrose to repress the promoter (no induction). Plates were incubated at 37 °C with 5% CO_2 and imaged. (*B*) GFP–MacP colocalizes with sites of TADA labeling at midcell. Strains AKF_Spn728, -326, and -730 were grown to midexponential phase in THY containing 0.2% fucose at 37 °C in 5% CO_2. Sites of active PG biogenesis were identified by incorporation of TADA for 15 min before imaging on 2% agarose pads. Representative images are shown $n = 3$. (Scale bar, 1 μm.) The slight reduction in cell width in the Δ*pbp1a* mutant is consistent with the data presented in Fig. S2 *A* and *B*. (*C*) Demographs showing enrichment of GFP–MacP at midcell. Cells expressing the GFP–MacP fusion (Δ*macP* P_{fuc}::*gfp-macP*) were prepared as in described above in *B*. Demographs show GFP and TADA fluorescence intensity profiles of the same 100 cells. Fluorescence profiles were normalized to the region of highest intensity for each cell to reduce signal heterogeneity, resulting profiles are collapsed to one pixel in width and plotted based on cell size. Approximately 50 cells are plotted per biological repeat, $n = 2$. Demographs were constructed using the open-source software package Oufti (1).

1. Paintdakhi A, et al. (2016) Oufti: An integrated software package for high-accuracy, high-throughput quantitative microscopy analysis. *Mol Microbiol* 9:767–777.

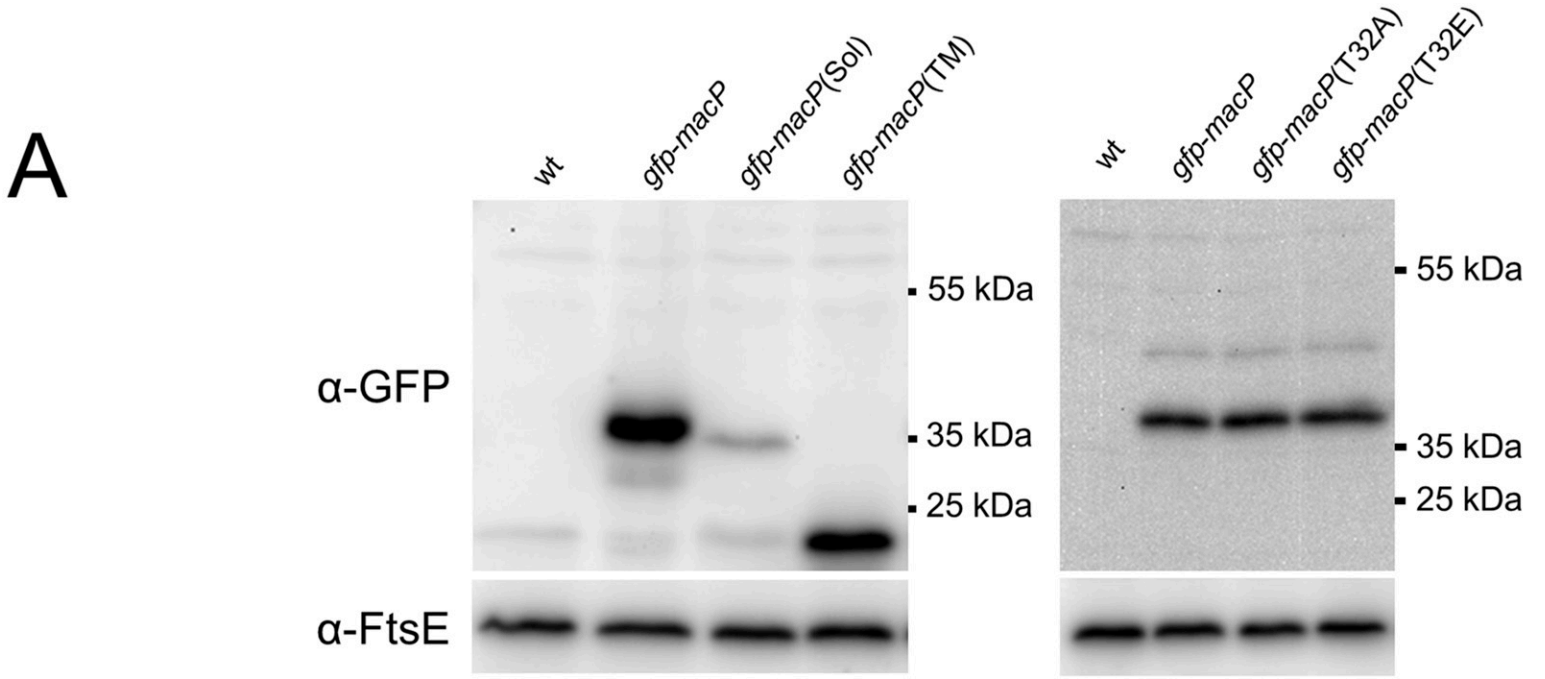

Fig. S5. Expression and complementation assays for GFP–MacP truncations. (*A*) Immunoblot analysis of strains expressing *gfp-macP* truncations under the control of a fucose-inducible promoter. Strains AKF_Spn740, -746, -750, -769, -771, and wild-type were grown to midexponential phase in THY +0.2% fucose at 37 °C in a 5% CO_2. Cultures were normalized to an OD_{600} of 0.3 before lysis. The anti-GFP immunoblot is representative three replicates. The anti-FtsE was used to control for loading. (*B*) GFP-MacP truncations and point mutants cannot complement the Δ*macP* Δ*pbp1a* synthetic lethality. The indicated *S. pneumoniae* strains were grown to exponential phase in the presence of 200 μM $ZnCl_2$ and normalized to an OD_{600} of 0.2. Resulting cultures were serially diluted and 5 μL of each spotted onto TSAII 5%SB plates containing 0.2% fucose in the presence or absence of 200 μM $ZnCl_2$. Plates were incubated at 37 °C in 5% CO_2 and imaged. Strains AKF_Spn764, -765, -766, -789, and -793 were used in these assays. Data are representative of two replicates. (*C*) Strains lacking PBP1a and expressing GFP–MacP(T32A) or GFP–MacP (T32E) have cell size defects consistent with loss of function. Midexponential phase cells for each strain were grown for 5 h 45 min in the presence of 0.2% fucose and either the presence or absence of 200 μM $ZnCl_2$. Cells were labeled with TADA for 15 min before imaging on 2% agarose pads. Strains AKF_Spn789 and -793 were compared with wild-type. Representative phase-contrast images are shown $n = 3$. (Scale bar, 3 μm.) (*D*) The GFP–MacP(T32A) and (T32E) variants are nonfunctional. Growth curves of cells lacking PBP1a and expressing GFP–MacP(T32A) or GFP–MacP(T32E) mirror aPBP depletion curves those shown in Fig. S2.

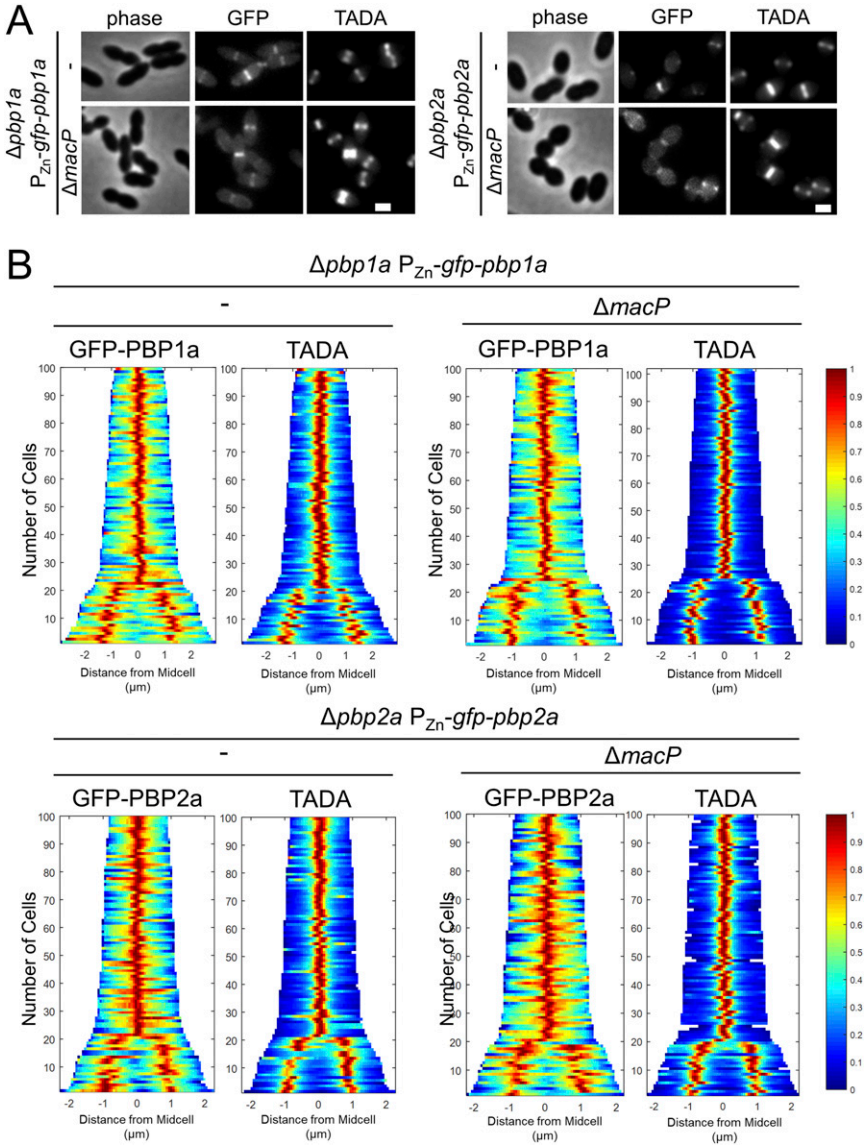

Fig. S6. GFP–PBP1a and GFP-PBP2a localize to sites of new PG synthesis independently of MacP. (*A*) The indicated strains were grown in THY 200 μM $ZnCl_2$ at 37 °C in 5% CO_2 to midexponential phase. Cells were labeled with TADA for 15 min before imaging on 2% THY agarose pads. Representative images of two replicates are shown. (Scale bar, 1 μm.) (*B*) Demographs of GFP–PBP1a and GFP–PBP2a in the presence and absence of MacP. Cells expressing the GFP–aPBP fusions were prepared as in described above in *A*. Demographs show GFP and TADA fluorescence intensity profiles of the same 100 cells. Fluorescence profiles were normalized to the region of highest intensity for each cell to reduce signal heterogeneity, resulting profiles are collapsed to one pixel in width and plotted based on cell size. Approximately 50 cells are plotted per biological repeat, $n = 2$. Demographs were constructed using the open-source software package Oufti (1).

1. Paintdakhi A, et al. (2016) Oufti: An integrated software package for high-accuracy, high-throughput quantitative microscopy analysis. *Mol Microbiol* 9:767–777.

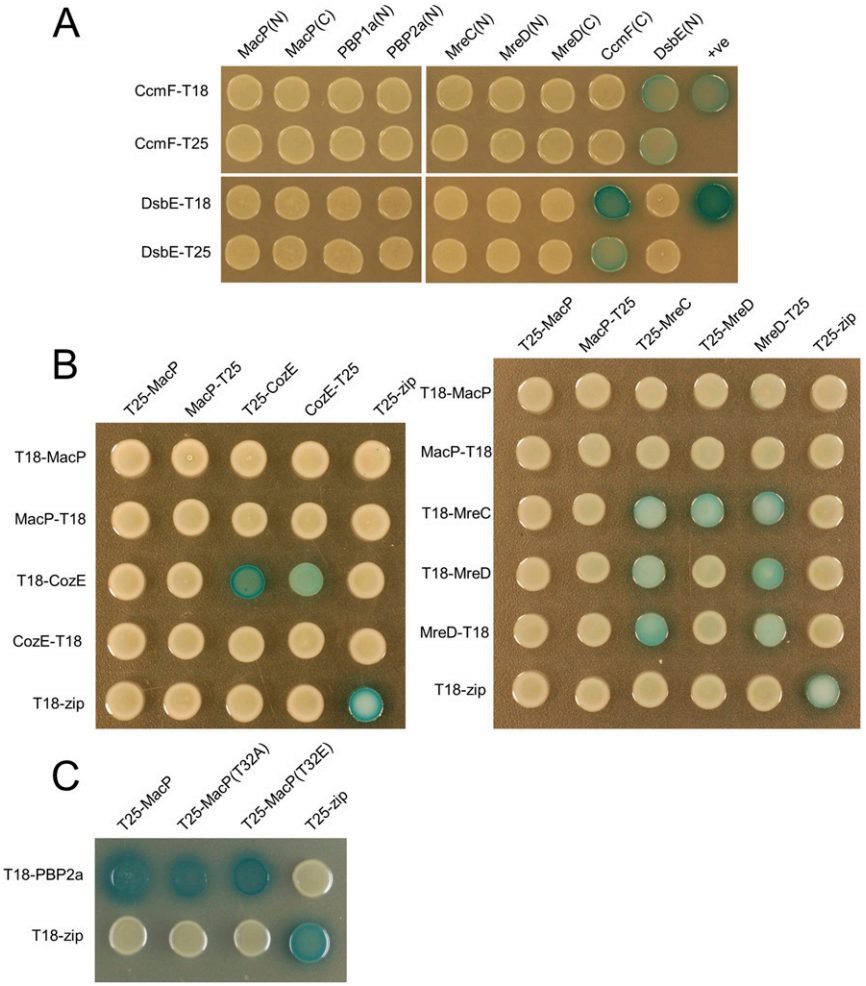

Fig. S7. Controls for the BACTH assay. BTH101 *E. coli* cells containing plasmids expressing indicated T18 and T25 protein fusions were grown to stationary phase in LB containing: Amp^{50} μg mL^{-1}, Kan^{25} μg mL^{-1}, and $IPTG^{500}$ μg mL^{-1}. Five-microliter of stationary phase culture was spotted onto LB agar containing: Amp^{50} μg mL^{-1}, Kan^{25} μg mL^{-1}, and X-gal^{40} μg mL^{-1}. Plates were incubated at 30 °C and imaged. The terminus used for T25 or T18 fusion to *S. pneumoniae* proteins are shown in parenthesis, (N) = N terminal or (C) = C terminal. The "zip" fusions are to a leucine zipper domain derived from the yeast protein GCN4 and serve as both positive and negative controls. (*A*) Specificity controls using DsbE and CcmF. Two *E. coli* membrane associated proteins that interact with each other. Representative images are shown of at least two biological replicates. (*B*) MacP does not give positive BACTH interactions with known members of the PG biosynthetic complex: CozE, MreC, or MreD. Representative images are shown of at least three biological replicates. (*C*) MacP(T32A) and MacP(T32E) retain their ability to interact with PBP2a. Representative images are shown of at least two biological replicates.

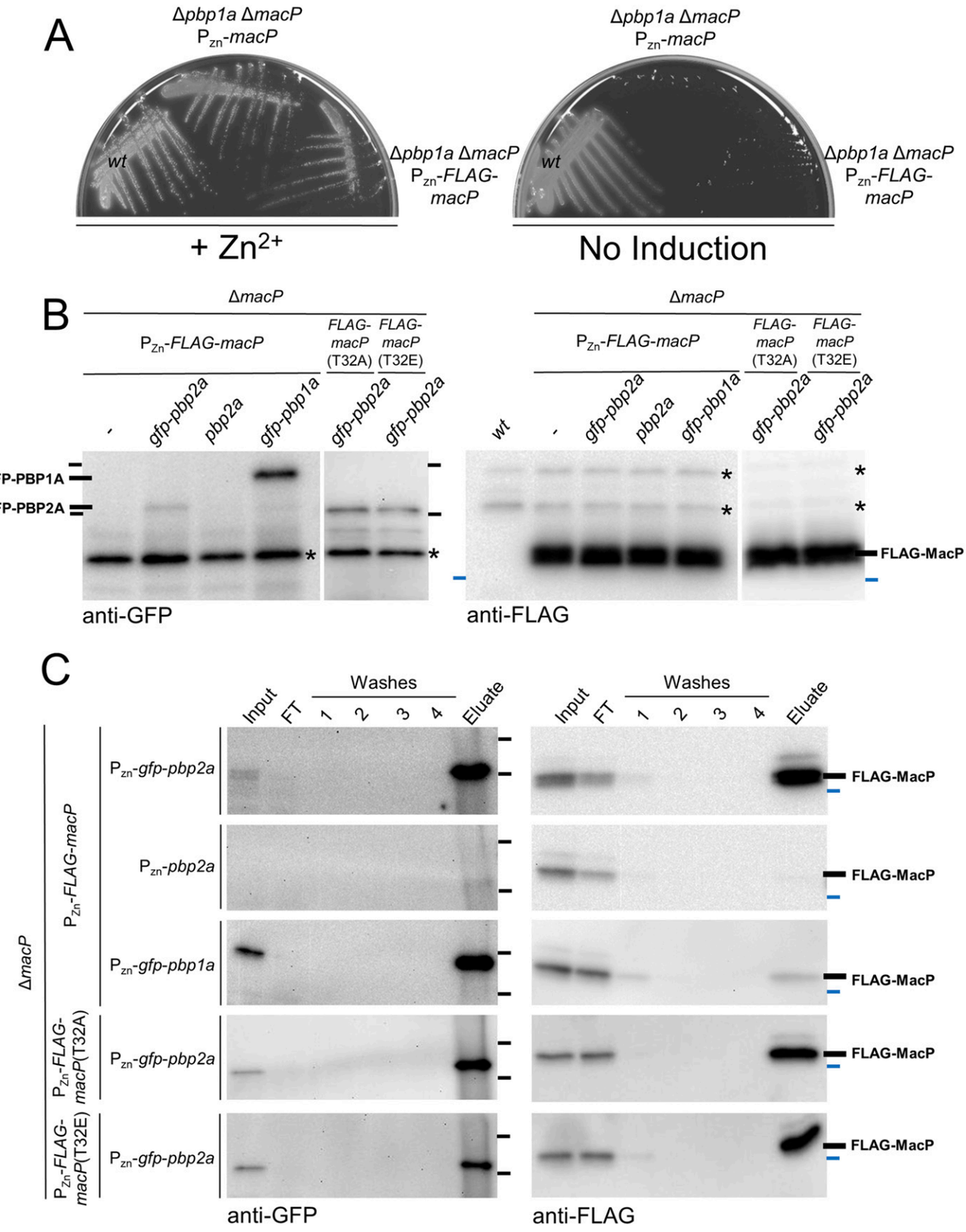

Fig. S8. Coimmunoprecipitation controls. (*A*) FLAG–MacP complements the Δ*pbp1A ΔmacP* synthetic lethality. Depletion strains contain *macP* or *FLAG-macP* fused to a Zn^{2+}-inducible promoter (P_{zn}). Strains were streaked on TSAII 5% SB overlay plates with or without 200 μM $ZnCl_2$. Plates were incubated at 37 °C with 5% CO_2 and imaged. The plate images shown are representative of two replicates. (*B*) Antibody specificity tests on whole cell lysates used for coimmunoprecipitation experiments. Midexponential phase cultures of the indicated strains grown in THY +400 μM $ZnCl_2$ at 37 °C with 5% CO_2. Cultures were normalized to an OD_{600} of 0.3 before lysis. Membranes were probed with monoclonal anti-GFP or monoclonal anti-FLAG antibodies. Nonspecific bands are highlighted with an asterisk (*). (*C*) Both aPBP enzymes reside in a complex with FLAG–MacP. Indicated strains were grown in the presence of 400 μM $ZnCl_2$. Membrane preparations were solubilized in 0.5% Digitonin. Solubilized membranes were incubated with an anti-GFP Sepharose resin for 4 h. The protein-bound resin was washed four times and bound proteins eluted in SDS/PAGE sample buffer. Indicated fractions were analyzed by immunoblot using monoclonal anti-GFP and anti-FLAG antibodies. FLAG–MacP, FLAG–MacP(T32A), and FLAG–MacP(T32E) coprecipitated with GFP–PBP2a. A smaller amount of FLAG–MacP coprecipitated with GFP–PBP1a. Representative blots are shown, $n = 3$. The position of protein markers are indicated by short marks to the right of each blot: 130 kDa and 100 kDa are shown in in black and the 15 kDa are indicated in blue.

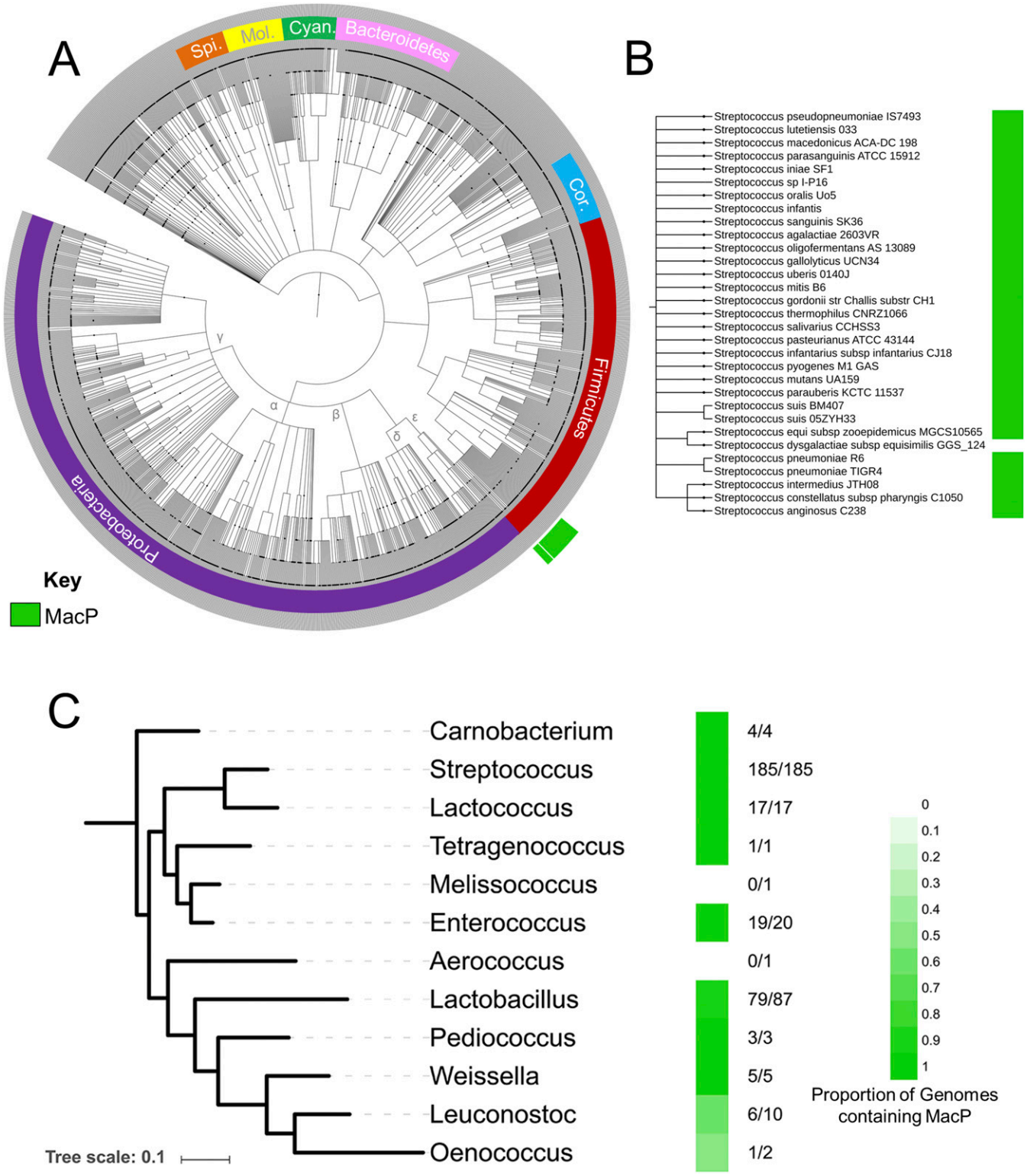

Fig. S9. MacP orthologs are present in the *Lactobacillales*. (*A*) Phylogenetic tree showing the presence of MacP *S. pneumoniae* homologs across 1,576 bacterial species. Species containing a MacP homolog are indicated by a green bar. Cor., *Corynebacteriales*; Cyan., *Cyanobacteria*; Mol., *Mollicutes*; and Spi., *Spirochaetae*. The tree was constructed using NCBI BLASTp, using the *S. pneumoniae* MacP protein sequence as the query to search against a database of bacterial genomes with an e-value cut-off of 1×10^{-4}. This analysis was carried out using the Harvard Medical School research computing cluster Orchestra (https://rc.hms.harvard.edu/#orchestra). The trees were drawn using the Interactive Tree Of Life (v3) web-based tool (itol.embl.de/) (1). (*B*) A section of the tree shown in *A*. (*C*) A more sensitive search for diverse homologs (see *SI Experimental Procedures*) indicates that MacP is present in *Lactobacillales*. The tree shows the genera that contain a MacP homolog. The number of species containing a MacP homolog compared with the total number of sequenced species in the genera are indicated.

1. Letunic I, Bork P (2007) Interactive tree of life (iTOL): An online tool for phylogenetic tree display and annotation. *Bioinformatics* 23:127–128.

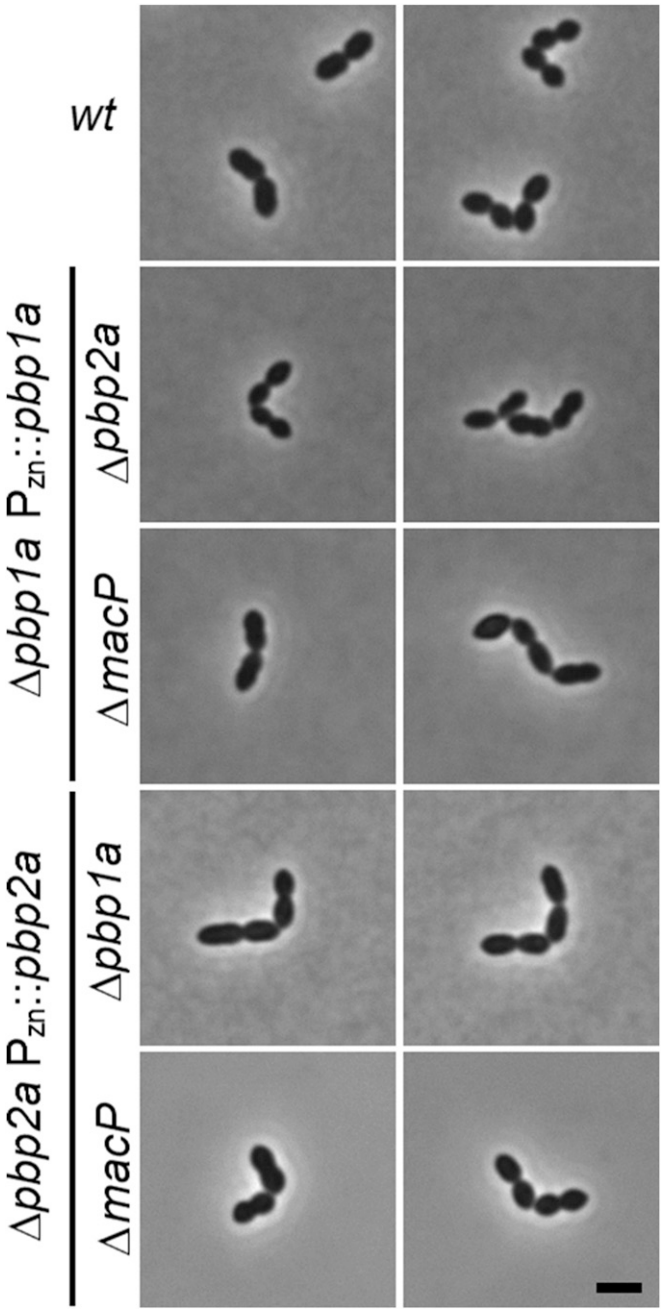

Movie S1. Cells depleted of essential aPBP activity undergo progressive cell size reduction and eventual lysis. Time-lapse movies of the indicated strains. Cells were grown to midexponential phase in the presence of 200 μM $ZnCl_2$ followed by dilution to an OD_{600} of 0.025 in fresh media without inducer. When the cultures reached an OD_{600} of ~0.2, cells were placed on a 2% THY agarose pad without inducer and transferred to a microscope preheated to 30 °C. Images were acquired every 5 min for ~8.5 h (100 cycles) and are shown at 10 frame per second. Two representative time-lapse series are shown for each strain and each series was performed at least twice. (Scale bar, 2 μm.)

Movie S1

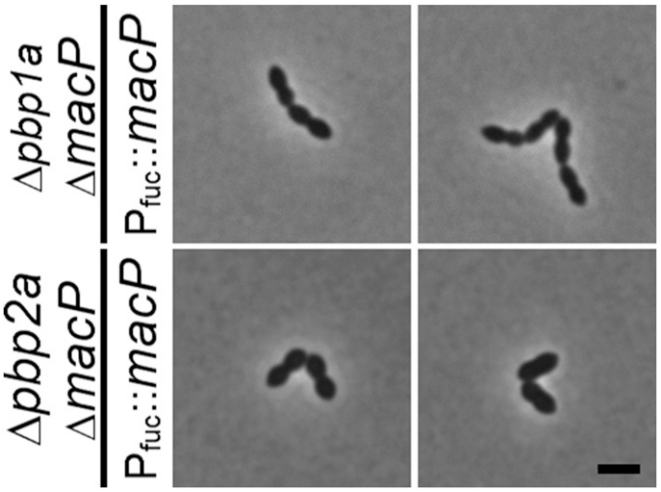

Movie S2. MacP depletion in strains lacking PBP1a show cell shape defects and lysis. Time-lapse movies of the indicated strains. Cell were grown to mid-exponential phase in the presence of 0.4% fucose followed by dilution to an OD_{600} of 0.025 in fresh media without inducer. When the cultures reached an OD_{600} of ~0.2, cells were placed on a 2% THY agarose pad without inducer and transferred to a microscope preheated to 30 °C. Images were acquired every 5 min for ~8.5 h (100 cycles) and are shown at 10 frames per second. Two representative time-lapse series are shown for each strain and each series was performed at least twice. (Scale bar, 2 μm.)

Movie S2

Other Supporting Information Files

Table S1 (DOCX)
Dataset S1 (DOCX)